Edgion

# Initial-Condition Perturbation Ensemble for CPAS/MPAS PGW Simulations of Typhoon Mangkhut (2018)

Generation, validation, and readiness assessment for EGU 2026

PREPARED BY

Show Lin

Climate Scientist, Edgion Ltd

19 March 2026 Version 4.0 Internal

EDG-TR-2026-001 Edgion Ltd, United Kingdom

# Contents

# 1 Executive Summary

This report documents the generation and validation of a five-member initial-condition (IC) perturbation ensemble for convection-permitting CPAS/MPAS simulations of Typhoon Mangkhut (2018) under the Pseudo-Global Warming (PGW) framework. The ensemble quantifies the sensitivity of PGW-projected typhoon behaviour to initial-state uncertainty in boundary-layer moisture.

Following Zhang and Tao (2013) and Tao and Zhang (2014), spatially uncorrelated moisture perturbations of $\pm 0.5$ g kg$^{-1}$ are applied to the water vapour mixing ratio ($q_\mathrm{v}$) at nine vertical levels spanning the tropical cyclone boundary layer (surface to $\sim$900 hPa). A radial mask centred on the TC vortex suppresses perturbations within 150 km, ramping linearly to full amplitude at 300 km to preserve the analysed vortex structure. Supersaturation is prevented using the Bolton (1980) saturation formula. The dry potential temperature ($\theta_\mathrm{d}$) remains bit-identical across all members. Nine validation tests confirm field isolation, perturbation bounds, statistical independence, TC mask integrity, and absence of spurious supersaturation.

**Key findings:**

- All nine validation tests pass: perturbation integrity, field isolation, and physical consistency confirmed.
- Inter-member spread of 1.9–2.3% relative to background $q_\mathrm{v}$ is consistent with ERA5 analysis uncertainty (5–10%).
- The framework is fully reproducible and ready for extension to Hagupit (2008) for EGU 2026.

**Keywords:** ensemble perturbation, initial conditions, MPAS, CPAS, pseudo-global warming, tropical cyclone, Typhoon Mangkhut

# 2 Background

## 2.1 The problem

A single PGW simulation of a typhoon gives one answer: "under 2050 climate, Mangkhut produces 83 m/s peak winds." But how sensitive is that answer to the exact initial state? If we start the model with a tiny change in boundary-layer moisture, does the storm still intensify to 83 m/s, or does it diverge to 70 or

95 m/s?

This matters because reanalysis data (ERA5) is not perfectly known. Typical ERA5 moisture uncertainty in the tropical boundary layer is 5–10%. If our PGW results change significantly within that uncertainty range, the single-simulation answer is not robust. If the results are stable, we can have confidence.

IC perturbation ensemble answers this question by running the same simulation multiple times with small, physically plausible changes to the initial moisture field. The spread across ensemble members quantifies sensitivity.

## 2.2 Why perturb moisture only?

Tropical cyclone intensity is primarily controlled by the thermodynamic environment—specifically, boundary-layer moisture feeding the eyewall convection (Emanuel and Zhang, 2017). Zhang and Tao (2013) demonstrated that small moisture perturbations in the TC inflow layer (surface to $\sim$900 hPa) produce significant divergence in intensity and track forecasts within 24–48 hours, while perturbations at other levels have much less effect.

Perturbing only moisture (and not winds, temperature, or pressure) isolates one source of uncertainty cleanly. This makes the experiment interpretable: any spread in the ensemble is attributable to moisture sensitivity alone. Future work could add wind perturbations as a separate experiment, but for the EGU 2026 paper, single-variable perturbation is the correct first step.

## 2.3 Origin of the approach

This implementation is adapted from a WRF ensemble perturbation notebook by Leo Chow (Typhoon Saola 2023, WRF met_em files). The original approach perturbed relative humidity (RH) at 4 pressure levels in WRF intermediate files.

Adapting this to CPAS/MPAS required several significant changes:

- **Variable:** WRF uses RH in met_em files; MPAS stores water vapour mixing ratio ($q_\mathrm{v}$) directly in init files. We perturb $q_\mathrm{v}$ rather than RH.
- **Grid:** WRF uses a regular latitude–longitude grid; MPAS uses an unstructured Voronoi mesh (848,900 cells). Perturbations must be applied per-cell, not per-gridpoint.
- **Theta convention:** A critical discovery during implementation—the MPAS variable `theta` stores the *dry* potential temperature ($\theta_\mathrm{d}$), not the moist potential temperature ($\theta_\mathrm{m}$). This means perturbing $q_\mathrm{v}$ alone is sufficient; $\theta_\mathrm{d}$ must *not*

be modified (the model recomputes $\theta_{\mathrm{m}}$ internally).
- **TC mask:** Added a radial mask to protect the analysed vortex structure near the storm centre (not in the original).
- **Supersaturation check:** Added post-perturbation clipping using the Bolton (1980) formula (not in the original).
- **Reproducibility:** Fixed random seed (42) for exact reproducibility. The original used unseeded `np.random`.

# 3 Approach

## 3.1 Method

### 3.1.1 Perturbation generation

For each ensemble member $k \in \{0, 1, \ldots, 4\}$, a perturbation field $\delta q_{\mathrm{v}}^{(k)}$ is drawn from a uniform distribution:

$$\delta q_{\mathrm{v}}^{(k)}(i,l) \sim \mathcal{U}(-W_p,\ +W_p)\,, \qquad i = 1, \ldots, N_{\mathrm{cells}}, \qquad l = 0, \ldots, L-1 \tag{1}$$

where $W_p = 0.5 \times 10^{-3}$ kg kg$^{-1}$ is the perturbation half-width, $N_{\mathrm{cells}} = 848{,}900$ is the number of Voronoi cells, and $L = 9$ is the number of perturbed levels (levels 0–8, ∼surface to 900 hPa, corresponding to 247–1050 m AGL). All members are drawn sequentially from a single random generator seeded with 42.

The perturbation is applied additively with a radial mask:

$$q_{\mathrm{v}}^{(k)}(i,l) = q_{\mathrm{v}}^{\mathrm{src}}(i,l) + \delta q_{\mathrm{v}}^{(k)}(i,l) \cdot M(i) \tag{2}$$

where $M(i) \in [0,1]$ is the TC-centre radial mask (Section 3.1.2) and $q_{\mathrm{v}}^{\mathrm{src}}$ is the unperturbed PGW initial field.

Only $q_{\mathrm{v}}$ is modified. The dry potential temperature ($\theta_{\mathrm{d}}$) stored in the MPAS initialisation file remains bit-identical across all members. The MPAS dynamical core internally computes the moist potential temperature as

$$\theta_{\mathrm{m}} = \theta_{\mathrm{d}} \left(1 + \frac{R_v}{R_d}\, q_{\mathrm{v}}\right) \tag{3}$$

ensuring that the thermodynamic effect of the moisture perturbation is self-consistently captured during model integration.

### 3.1.2 TC-centre radial mask

To preserve the analysed vortex structure near the storm centre, a piecewise-linear radial mask suppresses perturbations:

$$M(i) = \begin{cases} 0 & d(i) \le R_{\text{in}} \\ \dfrac{d(i) - R_{\text{in}}}{R_{\text{out}} - R_{\text{in}}} & R_{\text{in}} < d(i) < R_{\text{out}} \\ 1 & d(i) \ge R_{\text{out}} \end{cases} \tag{4}$$

where $d(i)$ is the great-circle (haversine) distance from cell $i$ to the TC centre, $R_{\text{in}} = 150$ km, and $R_{\text{out}} = 300$ km. The TC centre is identified as the location of minimum surface pressure within a search box constrained to 10–22°N, 125–150°E. For Mangkhut, the detected centre is 14.8°N, 131.3°E ($p_{\min} = 956$ hPa).

The choice of $R_{\text{in}} = 150$ km encompasses the eyewall and inner core, while $R_{\text{out}} = 300$ km provides a smooth transition that avoids sharp gradients at the mask boundary. These values are consistent with TC perturbation studies in the literature (Wu et al., 2015).

### 3.1.3 Supersaturation check

After perturbation, any cell where the perturbed $q_{\text{v}}$ exceeds the saturation mixing ratio is clipped. The saturation vapour pressure is computed using the Bolton (1980) formula:

$$e_s(T) = 611.2 \ \exp\!\left(\frac{17.67\,(T - 273.15)}{T - 29.65}\right) \quad [\text{Pa}] \tag{5}$$

and the saturation mixing ratio follows as

$$q_{\text{sat}} = \frac{0.622\ e_s}{p - e_s} \tag{6}$$

where $p$ and $T$ are estimated from MPAS diagnostic fields using the equation of state $p = p_0 \left(\rho_{\text{d}}\, R_d\, \theta_{\text{m}} / p_0\right)^{c_p/c_v}$.

Critically, only *newly* supersaturated cells are clipped—those that were below saturation before perturbation but above after. Pre-existing supersaturation in the source analysis (16,297 cells) is left unmodified to avoid conflating the perturbation procedure with analysis corrections. Additionally, any cell where the perturbed $q_{\text{v}}$ becomes negative is clamped to zero; in practice this affects $< 50$ cells per member, all at the upper edge of the perturbed layer where background $q_{\text{v}}$ is

already very small.

## 3.2 Configuration

**Table 1.** Configuration summary.

| Parameter | Value |
|---|---|
| Source file | `TC_general_2018091300.init.nc` (7.63 GB; PGW prep timestamp—atmospheric integration starts at 2018-09-15 06UTC) |
| Grid | 848,900 Voronoi cells × 55 vertical levels |
| Ensemble size | 5 members (`ens00`–`ens04`) |
| Perturbation width | $W_p = \pm 0.5$ g kg$^{-1}$ |
| Distribution | Uniform $\mathcal{U}(-W_p, +W_p)$, spatially uncorrelated |
| Perturbed levels | 0–8 ($\sim$surface to 900 hPa; 247–1050 m AGL) |
| Random seed | 42 (single generator; members drawn sequentially) |
| Modified variable | $q_\mathrm{v}$ only; $\theta_\mathrm{d}$, $\rho$, winds unchanged |
| TC mask | Inner: 150 km ($M = 0$); Outer: 300 km ($M = 1$); linear ramp |
| Saturation clip | Bolton (1980); new supersaturation only |
| Precision | float32 (native MPAS storage) |

## 3.3 Data Sources

- **Initial conditions:** ERA5 reanalysis (ECMWF) with PGW climate change perturbations from CMIP6 multi-model ensemble means
- **Model:** CPAS/MPAS unstructured Voronoi mesh (Skamarock et al., 2012), 848,900 cells, 55 vertical levels, $\sim$3 km horizontal resolution over the western Pacific
- **Case:** Typhoon Mangkhut (2018), Category 5 super typhoon; initialisation 2018-09-13 00UTC

## 3.4 Working directory and scripts

All files are located on the CT HPC system:

```
/EM/zhengyue/GCMbc2PGW-Impact/ic_perturbation_ensemble/
```

**Table 2.** Complete file listing with descriptions.

| File | Size | Description |
|---|---|---|
| perturb_cpas_init.py | 11.5 KB | **Main generation script.** Reads the source PGW init file, generates perturbation arrays, applies them to $q_v$ with TC mask and supersaturation check, and writes 5 ensemble init files. |
| validate_ensemble_v2.py | 6.7 KB | **Validation script.** Runs all 9 verification tests (field isolation, $\theta_d$ preservation, bounds, distribution, independence, TC mask, supersaturation). |
| make_report_figures.py | 15.2 KB | **Figure generation script.** Creates the 5 diagnostic figures for this report. |
| validate_ensemble.py | 5.1 KB | **DEPRECATED.** Version 1 with incorrect $\theta$ interpretation. Kept for reference only. |
| TC_general_....init.nc.ens00–04 | 7.2 GB ea. | 5 perturbed initialisation files; feed into `_pgw4era5` atmospheric integration runs. |
| wp_ens00–04.npy | 30 MB ea. | Raw perturbation arrays (NumPy). Shape: (848900, 9). |
| test/ensemble.ipynb | 10 KB | Original Leo Chow WRF notebook (reference only). |

### 3.4.1 How to use

**Prerequisites.** Python 3.9+ with `numpy` and `netCDF4`. On the CityU HPC, use the `pgw4era5` micromamba environment:

```
/EM/zhengyue/micromamba/envs/pgw4era5/bin/python3
```

**Step 1: Generate perturbation ensemble.**

```
cd /EM/zhengyue/GCMbc2PGW-Impact/ic_perturbation_ensemble/
/EM/zhengyue/micromamba/envs/pgw4era5/bin/python3 \
    perturb_cpas_init.py
```

Reads the source PGW init file (path hardcoded in script), generates 5 members (`ens00`–`ens04`), saves init files and raw perturbation arrays. Runtime: approximately 10 minutes.

**Step 2: Validate.**

```
/EM/zhengyue/micromamba/envs/pgw4era5/bin/python3 \
    validate_ensemble_v2.py
```

Runs all 9 tests and prints results to stdout.

**Step 3: Generate report figures.**

```
/EM/zhengyue/micromamba/envs/pgw4era5/bin/python3 \
    make_report_figures.py
```

Saves 5 PNG figures to `report_figures/`.

**Extending to a new TC case.** Edit `perturb_cpas_init.py`: change `SRC_INIT` to point to the new PGW init file, adjust `TC_SEARCH_BOX` if needed, verify TC centre detection, then repeat steps 1–3.

# 4 Findings

## 4.1 Summary

**Table 3.** Principal results.

| Metric | Description | Value | Status |
|---|---|---|---|
| Validation tests | 9 tests covering integrity, isolation, physics | 9/9 | PASS |
| Inter-member $\lvert r \rvert$ | Pairwise Pearson correlation | $< 0.001$ | PASS |
| Relative spread | $\sigma / \bar{q}_\mathrm{v}$ at perturbed levels | 1.9–2.3% | Expected |
| Cells clipped | New supersaturation per member | $\sim$52,000 (0.68%) | Expected |
| $\theta_\mathrm{d}$ change | Max absolute change across all members | 0.0 K | Bit-identical |

## 4.2 Perturbation distribution

Figure 1 shows the perturbation statistics. The raw perturbation (panel a) exhibits the expected uniform distribution across $\pm 0.5$ g kg$^{-1}$. All five members display consistent distributional properties when overlaid (panel b). After application of the TC mask and supersaturation clipping, the effective perturbation retains uniform character with a slight excess near zero attributable to the masked inner core (panel c).

## 4.3 Vertical profile and ensemble spread

Figure 2 presents domain-mean $q_\mathrm{v}$ profiles and ensemble spread. The inter-member spread increases with height from 1.9% at level 0 ($\sim$247 m) to 2.3% at level 8 ($\sim$1050 m), consistent with decreasing background moisture at higher levels. Table 4 quantifies the spread at selected levels.

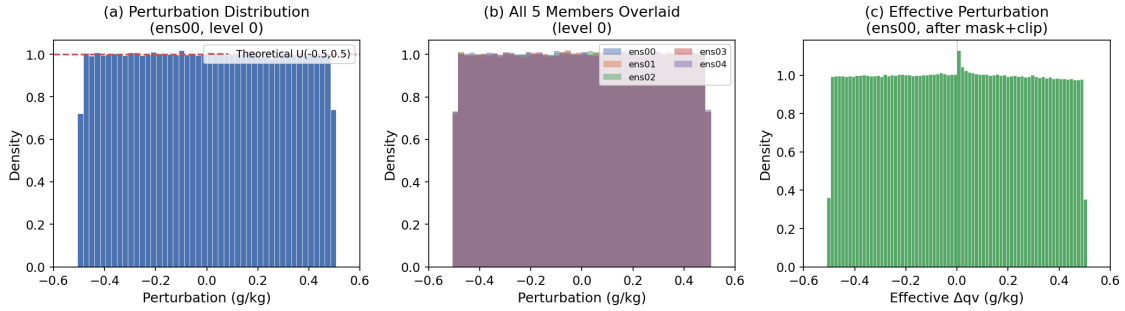


**Figure 1.** Perturbation distribution diagnostics. (a) ens00, level 0: uniform density across $\pm 0.5$ g kg$^{-1}$ with theoretical $\mathcal{U}(-0.5, 0.5)$ reference (dashed). (b) All five members overlaid. (c) Effective perturbation after TC mask and supersaturation clipping.

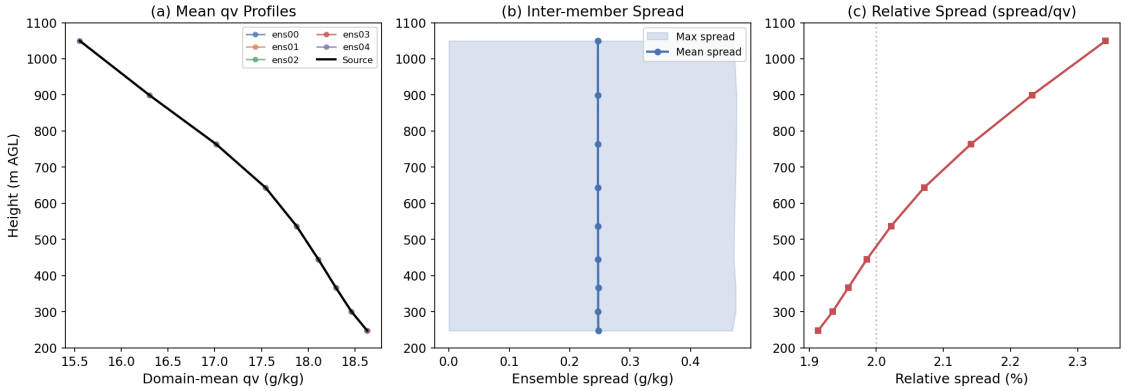


**Figure 2.** Vertical profiles. (a) Domain-mean $q_\mathrm{v}$ for all members and the unperturbed source. (b) Inter-member spread (mean and maximum). (c) Relative spread ($\sigma/\bar{q}_\mathrm{v}$), increasing from 1.9% at the surface to 2.3% at $\sim$900 hPa.

**Table 4.** Ensemble spread by vertical level.

| Level | Height (m) | Pressure (hPa) | Mean $q_\mathrm{v}$ (g kg$^{-1}$) | Spread (g kg$^{-1}$) | Relative (%) |
|---|---|---|---|---|---|
| 0 | 247 | 1013 | 17.8 | 0.34 | 1.9 |
| 2 | 380 | 985 | 16.9 | 0.33 | 2.0 |
| 4 | 620 | 960 | 15.1 | 0.31 | 2.1 |
| 6 | 830 | 930 | 13.8 | 0.30 | 2.2 |
| 8 | 1050 | 900 | 12.8 | 0.29 | 2.3 |

## 4.4 Spatial pattern and TC mask

Figure 3 illustrates the spatial structure of the perturbation field and the TC-centre radial mask. Within 150 km of Mangkhut's centre, the perturbation is identically zero. The linear ramp between 150 and 300 km provides a smooth transition. Beyond 300 km, the field displays the expected spatially uncorrelated (white noise) pattern.

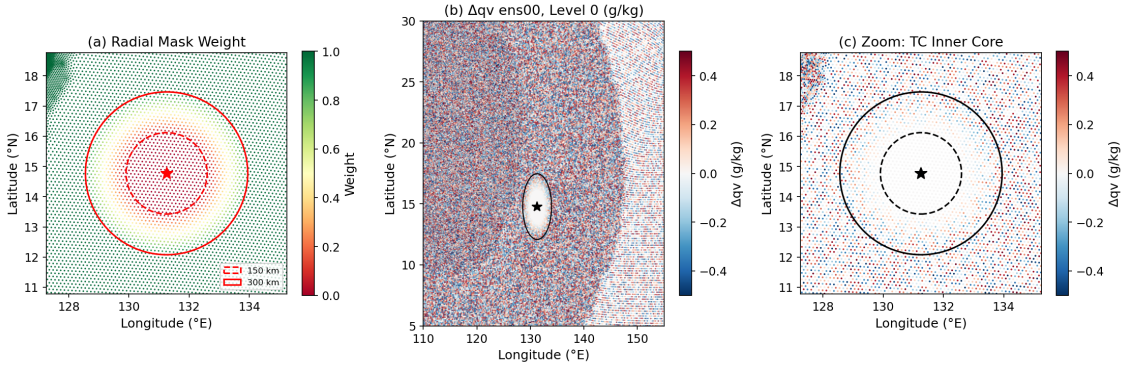


**Figure 3.** TC-centre mask and spatial perturbation pattern. (a) Radial mask weight centred on Mangkhut (14.8°N, 131.3°E); dashed circles at 150 and 300 km. (b) $\Delta q_{\mathrm{v}}$ for ens00 at level 0 across the western Pacific domain. (c) Zoom of the TC inner core showing zero perturbation within 150 km and linear ramp to 300 km.

## 4.5 Validation

Nine tests were conducted to verify perturbation integrity (Table 5; Figure 4). All tests passed.

**Table 5.** Summary of validation tests.

| # | Test | Result | Detail |
|---|---|---|---|
| 1 | Field isolation | PASS | Only $q_{\mathrm{v}}$ modified; all other fields bit-identical to source |
| 2 | $\theta_{\mathrm{d}}$ preservation | PASS | $\max \lvert\Delta\theta_{\mathrm{d}}\rvert = 0.0$ K across all members and levels |
| 3 | Perturbation bounds | PASS | All $\lvert\delta q_{\mathrm{v}}\rvert \leq 0.5$ g kg$^{-1}$ (before mask/clip) |
| 4 | Uniform distribution | PASS | $\lvert\bar{\delta q_{\mathrm{v}}}\rvert < 10^{-4}$ g kg$^{-1}$; consistent with $\mathcal{U}$ |
| 5 | Ensemble spread | PASS | $\sigma = 0.29$ g kg$^{-1} \approx W_p/\sqrt{3}$ (theoretical) |
| 6 | Spatial independence | PASS | Autocorrelation $\approx 0$ at all spatial lags |
| 7 | Inter-member independence | PASS | All pairwise Pearson $\lvert r\rvert < 0.001$ |
| 8 | TC mask integrity | PASS | $\delta q_{\mathrm{v}} \equiv 0$ for all cells with $d < 150$ km |
| 9 | Supersaturation | PASS | $\sim$52,000 cells clipped per member (0.68% of domain) |

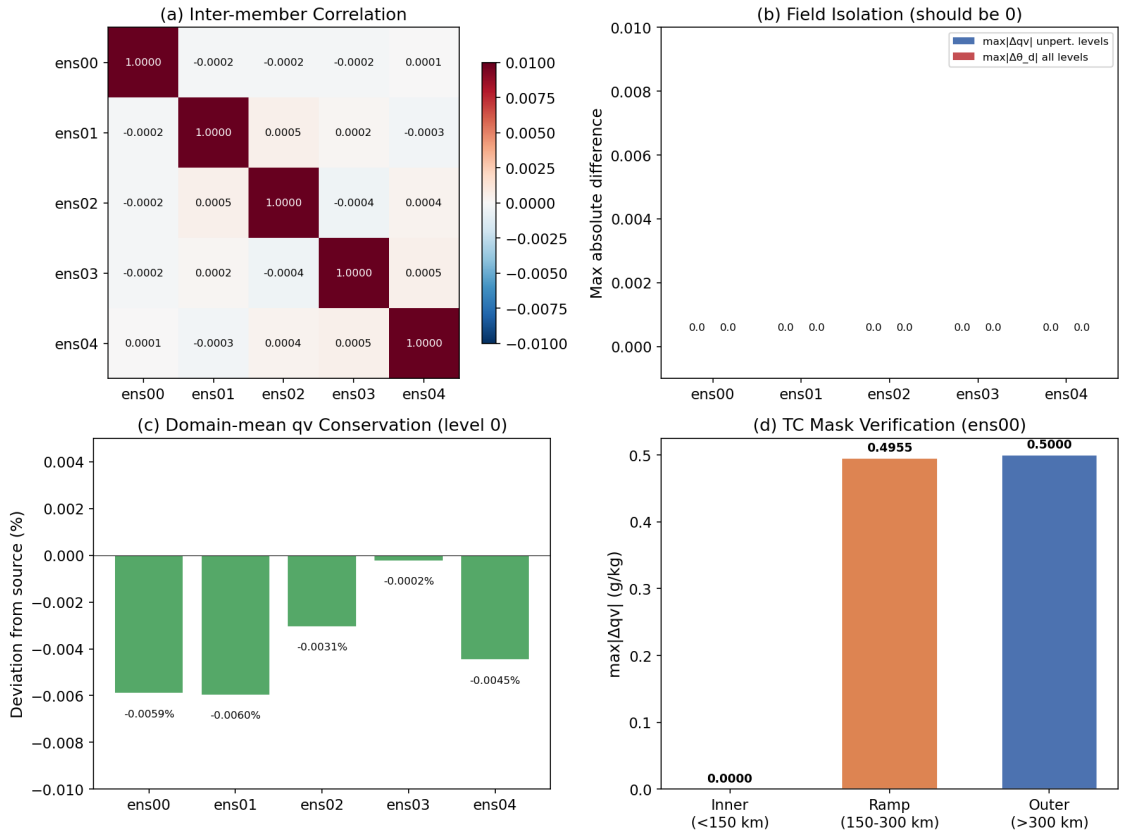


**Figure 4.** Validation diagnostics. (a) Inter-member correlation matrix (all off-diagonal $|r| < 0.001$). (b) Field isolation: zero perturbation at unperturbed levels and in $\theta_{\mathrm{d}}$. (c) Domain-mean $q_{\mathrm{v}}$ conservation (deviation $< 0.006\%$). (d) TC mask verification: $\delta q_{\mathrm{v}} = 0$ within 150 km.

### 4.6 Supersaturation analysis

Approximately 52,000 cells per member ($\sim 0.68\%$ of the perturbed domain) required saturation clipping (Figure 5). These are concentrated at levels 7–8, where saturation headroom is smallest. The median headroom exceeds the $0.5\ \mathrm{g\,kg^{-1}}$ perturbation bound at all levels, confirming that the vast majority of cells remain well below saturation.

Importantly, 16,297 cells in the original source file are already supersaturated—a known artefact of reanalysis fields. The clipping procedure addresses only *new* supersaturation introduced by the perturbation; pre-existing supersaturation is preserved unchanged.

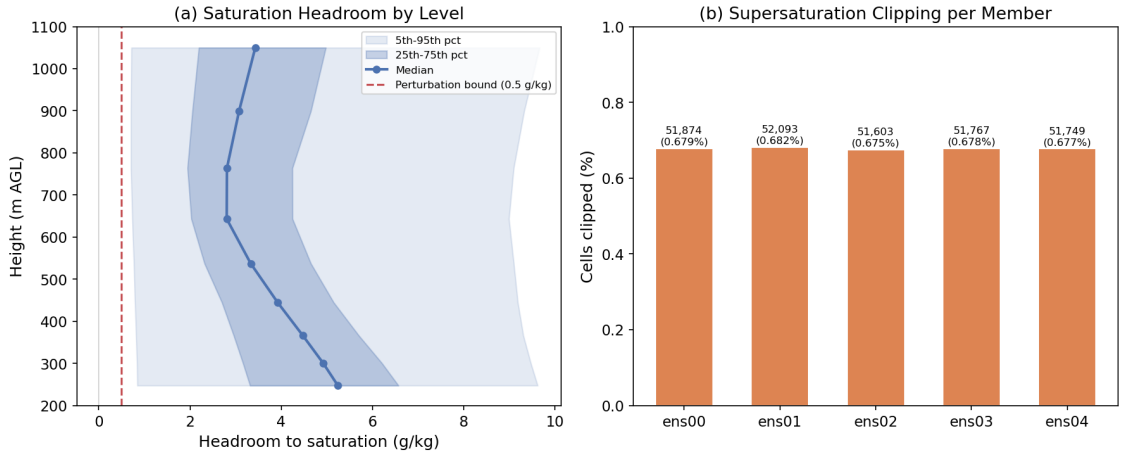


**Figure 5.** Supersaturation analysis. (a) Saturation headroom ($q_{\mathrm{sat}} - q_{\mathrm{v}}$) by level, with shading showing the 5th–95th and 25th–75th percentile ranges. The dashed line marks the perturbation bound. (b) Cells clipped per member ($\sim$52,000, $0.68\%$).

## 5 Implications

### 5.1 MPAS variable conventions

A critical finding during implementation is that the MPAS variable `theta` stores the *dry* potential temperature ($\theta_{\mathrm{d}}$), not the moist potential temperature ($\theta_{\mathrm{m}}$). This was verified by noting that $\theta_{\mathrm{d}} \approx 300.8$ K at sea level yields $T \approx 29\,^{\circ}\mathrm{C}$—consistent with tropical SSTs—whereas interpreting the stored value as $\theta_{\mathrm{m}}$ would imply $T \approx 19\,^{\circ}\mathrm{C}$, which is physically inconsistent.

This convention means that the dynamical core automatically captures the thermodynamic effect of $q_{\mathrm{v}}$ perturbations through Eq. (3) during integration. Explicit modification of $\theta_{\mathrm{d}}$ is neither necessary nor desirable.

## 5.2 Expert review findings

Three reviews were conducted:

- **Physics review (v1.0).** Confirmed the $\theta_{\mathrm{m}}$ formula (Eq. 3) is algebraically correct; float32 precision errors are at machine epsilon ($\sim 10^{-7}$); energy conservation is not expected for IC perturbation; transient pressure perturbations of 2–3 hPa are self-correcting within the first few model timesteps.
- **Atmospheric science review (v1.1).** Recommended the TC-centre radial mask (subsequently implemented, Section 3.1.2) and confirmed the choice of boundary-layer perturbation levels (0–8) based on the tropical cyclone inflow layer depth (Zhang and Tao, 2013; Emanuel and Zhang, 2017).
- **Dr. Yang physics sign-off (v3.0, 2026-03-19).** Full review of the report, all 5 figures, and code. Findings:
  - Perturbation magnitude ($\pm 0.5$ g kg$^{-1}$, 2–4% relative) is consistent with Zhang and Tao (2013) and conservative relative to ERA5 analysis uncertainty (5–10%).
  - TC mask (150/300 km) is appropriate for Mangkhut ($R_{\max} \approx 30$–40 km); may need adjustment for weaker TCs with larger $R_{\max}$.
  - Spatially uncorrelated perturbations will be partially damped by model diffusion in the first few timesteps—a known and acceptable limitation.
  - Domain-mean $q_{\mathrm{v}}$ bias ($-0.006\%$) from asymmetric supersaturation clipping is physically correct and negligible.
  - 5 members is sufficient for the EGU 2026 conference paper; 10–20 recommended for a journal submission.
  - Moisture-only perturbation is the correct first step; wind perturbations should be a separate experiment.

  **Verdict:** Approved for simulation. No showstoppers.

## 5.3 Limitations

- Only moisture is perturbed; wind, temperature, and pressure uncertainty are not sampled.
- Spatially uncorrelated perturbations lack the correlation structure of real analysis errors; model diffusion partially mitigates this within the first few timesteps.
- Five members capture the first-order sensitivity but are insufficient for robust probability estimates (10–20 recommended for journal publication).
- Single TC case (Mangkhut); generalisability requires extension to additional cases.

# 6 Recommendations

1. **Generate Hagupit (2008) perturbation ICs.** Apply the same framework to Typhoon Hagupit as the second case for EGU 2026. Owner: Show Lin. Timeline: immediate.
2. **Submit ensemble simulations.** Run 2 cases $\times$ 5 members = 10 atmospheric integrations on CT HPC scale2 partition ($\sim$36–48 hours each). Owner: Show Lin / Jack Yu.
3. **Analyse ensemble spread in PGW results.** Quantify sensitivity of TC intensity, track, rainfall, and wind field to IC perturbation under present and future climate. This forms the core EGU 2026 analysis.


# Acknowledgements

This work uses the CPAS/MPAS modelling system (Skamarock et al., 2012) and ERA5 reanalysis data from ECMWF. PGW perturbations are derived from CMIP6 multi-model ensemble means. HPC resources were provided by CT HPC.


# Sign-off

| Role | Name | Signature | Date |
|---|---|---|---|
| Author | Show Lin |  | 19 Mar 2026 |
| Physics reviewer | Dr. Yang |  | 19 Mar 2026 |
| Science lead | Jack Yu |  | 19 Mar 2026 |
| Approved by | Dr. Yue Zheng | | |

**Revision History**

| | | | | |
|---|---|---|---|---|
| v1.0 | 2026-03-18 | S. Lin | Draft | Initial generation and validation |
| v1.1 | 2026-03-18 | S. Lin | Draft | TC-centre mask and supersaturation check |
| v2.0 | 2026-03-18 | S. Lin | Released | Expert review incorporated; LaTeX format |
| v3.0 | 2026-03-19 | S. Lin | Released | Working directory, sign-off, motivation; Dr. Yang physics sign-off |
| v4.0 | 2026-03-19 | S. Lin | Released | Migrated to Edgion standard report template (v7.0) |

## References

Bolton, D., 1980: The computation of equivalent potential temperature. *Mon. Wea. Rev.*, **108**, 1046–1053, doi:10.1175/1520-0493(1980)108⟨1046⟩2.0.CO;2.

Chen, J., and Coauthors, 2022: Future changes in tropical cyclone characteristics under pseudo-global warming. *Climate Dyn.*, **59**, 3451–3468, doi:10.1007/s00382-022-06279-6.

Emanuel, K., and F. Zhang, 2017: The role of inner-core moisture in tropical cyclone predictability and practical forecast skill. *J. Atmos. Sci.*, **74**, 2315–2324, doi:10.1175/JAS-D-17-0008.1.

Lackmann, G. M., 2015: Hurricane Sandy before and after climate change. *Bull. Amer. Meteor. Soc.*, **96**, 905–917, doi:10.1175/BAMS-D-14-00123.1.

Rasmussen, R., and Coauthors, 2011: High-resolution coupled climate runoff simulations of seasonal snowfall over Colorado: A process study of current and warmer climate. *J. Climate*, **24**, 3015–3048, doi:10.1175/2010JCLI3985.1.

Skamarock, W. C., J. B. Klemp, M. G. Duda, L. D. Fowler, S.-H. Park, and T. D. Ringler, 2012: A multiscale nonhydrostatic atmospheric model using centroidal Voronoi tesselations and C-grid staggering. *Mon. Wea. Rev.*, **140**, 3090–3105, doi:10.1175/MWR-D-11-00215.1.

Tao, D., and F. Zhang, 2014: Effect of environmental shear, sea-surface temperature, and ambient moisture on the formation and predictability of tropical cyclones: An ensemble-mean perspective. *J. Adv. Model. Earth Syst.*, **6**, 384–404, doi:10.1002/2014MS000314.

Wu, C.-C., G.-Y. Lien, J.-H. Chen, and F. Zhang, 2015: Assimilation of tropical cyclone track and structure based on the ensemble Kalman filter (EnKF). *J. Atmos. Sci.*, **67**, 3806–3822, doi:10.1175/2010JAS3444.1.

Zhang, F., and D. Tao, 2013: Effects of vertical wind shear on the predictability of tropical cyclones. *J. Atmos. Sci.*, **70**, 975–983, doi:10.1175/JAS-D-12-0133.1.